

On the phase transition in CsCN

G. Knopp, K. Knorr, Alois Loidl, S. Haussühl

Angaben zur Veröffentlichung / Publication details:

Knopp, G., K. Knorr, Alois Loidl, and S. Haussühl. 1983. "On the phase transition in CsCN." *Zeitschrift für Physik B Condensed Matter* 51 (3): 259–63.
<https://doi.org/10.1007/bf01307681>.



On the Phase Transition in CsCN

G. Knopp, K. Knorr, and A. Loidl

Institut für Physik der Universität, Mainz, Federal Republic of Germany

S. Haussühl

Institut für Kristallographie, Universität zu Köln, Federal Republic of Germany

X-ray diffraction and dielectric measurements have been performed on the molecular crystal CsCN as a function of temperature. The order parameter of the cubic to rhombohedral phase transition ($T_c=186$ K) was determined and interpreted by a coupling of the $(\text{CN})^-$ orientations to the shear strain. At lower temperatures the dielectric response is dominated by thermally activated relaxations processes rather than by electrical ordering of the CN dipoles.

1. Introduction

CsCN crystallizes in the cubic CsCl-structure in which the aspherical $(\text{CN})^-$ ions are orientationally disordered. At about 190 K it transforms into a rhombohedral structure [1, 2]. Specific heat measurements [3] showed that the entropy change connected with this structural phase transition is $R \cdot \ln 4$ suggesting that the axes of the CN molecules align along one of the $\langle 111 \rangle$ directions. The molecules are thought to remain disordered with respect to head and tail, in particular since no second specific heat anomaly was observed down to low temperatures.

Recent inelastic neutron scattering and ultrasonic results in the cubic phase proved the existence of rotational excitations of the CN molecules which via the coupling to the acoustic phonon branches drive the ferroelastic transition [4, 5]. This concept is also supported by molecular dynamics calculations [6].

Owing to the different crystal structure CsCN is an attractive alternative to the NaCl-type alkali cyanides KCN, NaCN, RbCN where the structural and dynamical properties have been studied in great detail [7].

In the present article we will report X-ray diffraction and dielectric results on CsCN and will comment on the cubic to rhombohedral phase transition and on the dipolar relaxation in the low temperature phase.

2. Experimental Results

Single crystals of CsCN were grown from the melt employing the Czochralski method. The X-ray measurements were performed on a two circle diffractometer using the Cu-K_α radiation. The samples were protected against moisture and were mounted into a variable temperature nitrogen cryostat equipped with Mylar windows.

For the dielectric measurements a single crystal, 2 mm thick and a cross section of 50 mm^2 was fixed between two flat capacitor plates, the [100] direction being parallel to the electric field. The real and imaginary part of the dielectric response was determined at frequencies of 100, 200, 400 Hz, 1, 2, 4, 10, 20, 40 and 100 kHz using an automated LCR-meter with an excitation voltage of 1 V.

2.1. X-Ray Diffraction

The X-ray investigation was started by recording 2θ -scans on a pulverized sample. Two spectra characterizing the cubic high temperature and the low temperature phase are shown in Fig.1. Here the intensities are already corrected for the background scattering from the sample holder. The high temperature data are consistent with a simple cubic lattice ($T=295$ K: $a=4.28$ Å), the low temperature data can be explained by a rhombohedral structure which

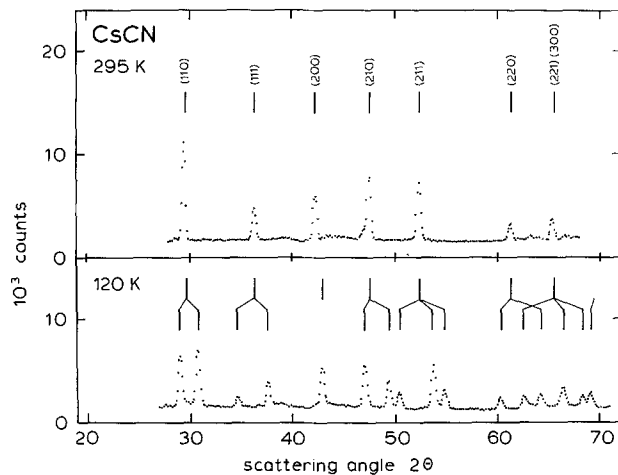


Fig. 1. The powder spectra of CsCN in the cubic and in the rhombohedral phase

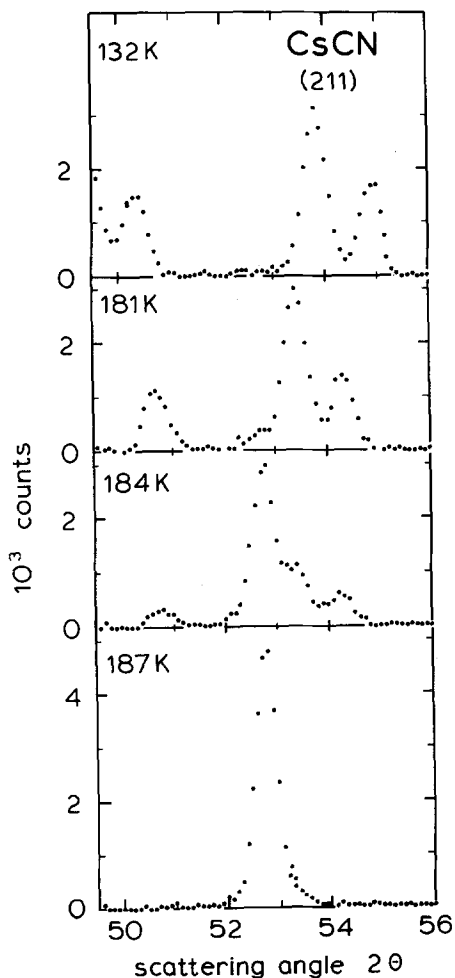


Fig. 2. 2θ -scans through the (211) Debye-Scherrer-line of a powdered CsCN sample

results from the stretching of the cubic cell along one of the $\langle 111 \rangle$ directions ($T=130$ K: $a=4.23$ Å, $\alpha=86.31^\circ$).

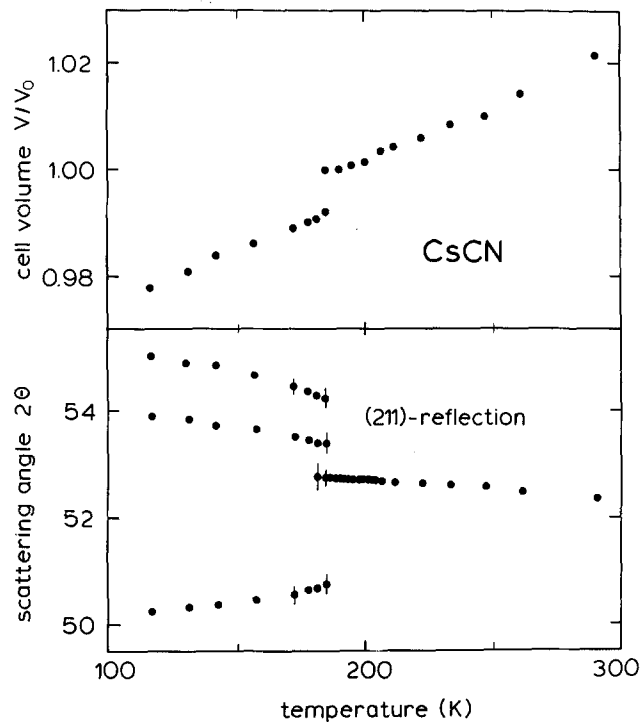


Fig. 3. The peak positions of the (211) Debye-Scherrer-line and the cell volume of CsCN as a function of temperature. V_0 is the volume of the cubic cell just above T_c

The splitting of the cubic powder lines is indicated.

The temperature dependence of some reflections of the single crystal and of some Debye Scherrer lines of the powdered sample were studied in more detail. Figure 2 shows scans of the (211) powder line. As can be seen the cubic line and the three rhombohedral lines coexist at temperatures close to the critical temperature T_c . The peak positions were determined by fitting routines, the result is shown in Fig. 3. One notes a jump to a finite splitting at $T_c=(186 \pm 1)$ K. The cell parameter α which is the angle between the primitive translation of the lattice and the cell volume V were calculated from the peak positions. The quantity $\Delta\alpha$, $\Delta\alpha=90-\alpha$, can be regarded as the order parameter of the phase transition, it is shown in Fig. 4 as a function of temperature. Here we also included values derived from the splitting of the (001) Bragg reflection of the single crystal. Obviously the powdered sample and the single crystal give identical results.

The phase transition is accompanied by a discontinuous contraction of the cell volume of about two percent (Fig. 3). There is, however, no tetragonal component of the cell deformation since the (h00) reflections fail to exhibit any splitting or broadening upon the transition.

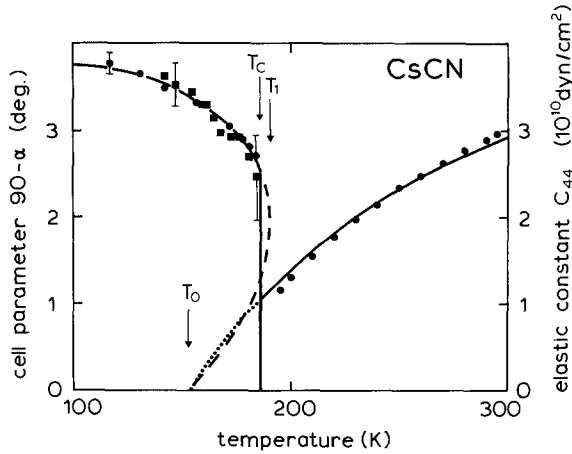


Fig. 4. The cell parameter $90-\alpha$, where α is the angle between the crystal axes, and the elastic constant c_{44} of the cubic phase versus temperature. For $T > T_c$: elastic constant c_{44} (●). For $T < T_c$: cell parameter $90-\alpha$ (powder sample (●), single crystal (■)). $90-\alpha$ and c_{44} can be regarded as the order parameter and the conjugate inverse susceptibility of the cubic to rhombohedral phase transition. The solid lines are the result of a mean field theory described in the text. The dashed and dotted lines represent the unphysical continuation of the mean field results

As the form factor of C and N are very small compared to the form factor of Cs there is no chance to determine the CN-orientations in either phase from X-ray experiments. We therefore used a study of the dielectric properties to gain insight into the CN-system. Nevertheless we want to mention that our X-ray results on the cubic phase revealed a special type of anisotropy of Bragg intensities. Calling the average intensity of the $\{300\}$ reflections $I\{300\}$ etc. we observed that the ratios $I\{300\}/I\{122\}$, $I\{033\}/I\{411\}$, $I\{511\}/I\{333\}$ and $I\{522\}/I\{144\}$ were systematically smaller than unity. An analysis in terms of an anisotropic Debye-Waller-factor of Cs leads to larger mean square displacements along $\langle 100 \rangle$ than $\langle 111 \rangle$ presumably as a consequence of the probability distribution of the CN-orientations which is believed to have maxima along $\langle 111 \rangle$.

2.2. Dielectric Measurements

Figure 5 shows the temperature dependence of the real and imaginary part, ϵ' and ϵ'' , of the dielectric constant of CsCN for 1 and 100 kHz. The results obtained with different frequencies coincide except for temperatures between 50 K and 100 K where also a finite loss becomes apparent. As usual the loss maximum is shifted to lower temperatures for lower frequencies.

The reduction of the orientational degrees of freedom from 8 to 2 at the 186 K phase transition shows up as a step in ϵ' . Here we assume that the $\langle 111 \rangle$

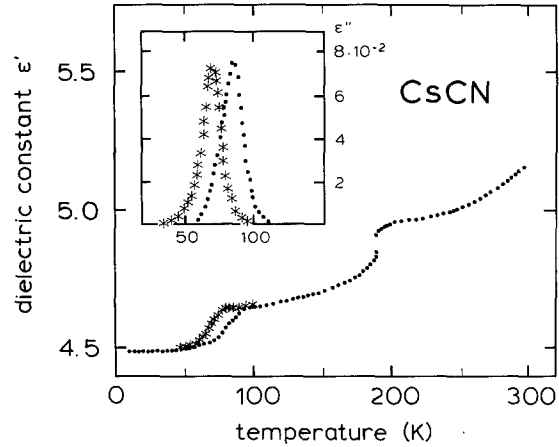


Fig. 5. The temperature dependence of the real and the imaginary part of the dielectric constant ϵ' and ϵ'' of CsCN. For better clarity the results of only two measuring frequencies are included: 1 kHz (*), 100 kHz (●). The appearance of dispersion and of noticeable dielectric loss is restricted to a temperature range between 60 K and 90 K

model for the CN-orientations in the cubic phase as proposed by molecular dynamics calculations and the specific heat anomaly is correct. Below the transition temperature the two degrees of freedom remaining are expected to lead to a Curie-Weiß type behaviour of the static dielectric constant $\epsilon_0(T)$ and eventually to an electrical ordering. On the other hand it is evident that a CN-molecule when performing reorientations between the $[111]$ and the $[\bar{1}\bar{1}\bar{1}]$ direction not only has to adjust to the mean dipolar field imposed by its neighbours but also has to pass a hindering potential barrier, an effect which is essential when discussing results obtained at finite frequencies.

The present data fail to show a clear cut Curie-Weiß-temperature dependence, but they exhibit a second reduction of the dielectric constant ϵ' between 50 K and 100 K which is connected with a high dielectric loss. This behaviour is an indication for the existence of thermally activated reorientation processes. The T -dependence of ϵ is then given by Debye's expression combined with an Arrhenius law for the reorientation time $\epsilon(T) = \epsilon_0(T)/(1 - i\omega\tau)$ with $\tau = \tau_0 \exp(E/kT)$. Figure 6 gives an evaluation of the maximum of the dielectric loss as a function of frequency ν and temperature. Figure 6a (ω versus T^{-1}) yields an attempt frequency τ_0^{-1} of $1.73 \cdot 10^{14}$ Hz and a hindering barrier E of 1,690 K (similar results have been reported by F. Lütty [7]). Figure 6b (ϵ''_{\max} versus T) shows that the static dielectric constant $\epsilon_0(T)$ is almost constant with slight decrease with falling temperature. Note that this

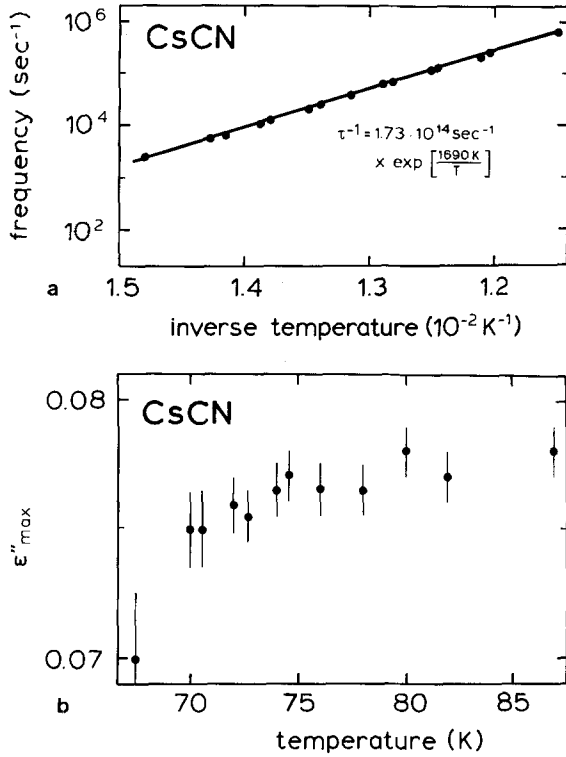


Fig. 6a and b. Evaluation of dielectric loss data in CsCN in the 60–90 K range: **a** Logarithmic plot of the frequency of maximum loss vs inverse temperature; **b** Plot of the maximum height of the dielectric loss ϵ''_{\max} versus temperature

type of evaluation is possible in the narrow temperature range only where finite loss was observed. Summarizing, one finds that the dielectric response is dominated by reorientations whose T -dependent rates pass the frequency window of the experiment at 60 K to 90 K. The static dielectric constant is rather constant or slightly decreasing than increasing to lower temperatures.

3. Discussion

It is clear that the cubic to rhombohedral phase transition in CsCN is induced by a coupling of the $(\text{CN})^-$ reorientations to the lattice strains. A direct proof for this rotational translational coupling was given by our recent inelastic neutron scattering experiments [4, 5] which showed an interaction of low lying orientational excitations of the CN-dumbbells with transverse acoustic phonons. The softening of the transverse phonons was found to be stronger in T_{2g} than in E_g symmetry. The temperature dependence of the elastic constant c_{44} in the cubic high temperature phase is reproduced in Fig. 4 [5]. The spontaneous rhombohedral shear $\Delta\alpha$ and the elastic constant c_{44} can be regarded as order param-

eter and conjugate inverse susceptibility of the structural phase transition in CsCN at 186 K. Following Shinnaka et al. [8], Blat and Zinenko [9] or De Raedt et al. [10] the free energy of the coupled system can be written within mean field approximation in lowest order as

$$F = \frac{1}{2}c_{44}^0(\Delta\alpha)^2 + C \cdot s \cdot (\Delta\alpha) + k_B T \left[\frac{2(1+3s)}{8} \cdot \ln \frac{1-3s}{8} + 2 \frac{3}{8} (1-s) \cdot \ln \frac{1-s}{8} \right].$$

Here c_{44}^0 is the background elastic constant of the lattice decoupled from the molecular excitations, $\Delta\alpha$ is the T_{2g} strain along the [111] direction, C the rotational-translational coupling constant and s is the order parameter of the $(\text{CN})^-$ orientations. The first term describes the elastic energy of the deformed lattice, the second one a bilinear coupling of the lattice with the dumbbell orientations and the last one the entropy of the $(\text{CN})^-$ system. The probabilities for $(\text{CN})^-$ ions pointing along one of the eight $\langle 111 \rangle$ directions are given by $(1+3s)/8$ for [111] and $[\bar{1}\bar{1}\bar{1}]$ and by $(1-s)/8$ for the other six directions. The model ignores the interaction of the dumbbell reorientations to E_g strains (for which there is no experimental evidence) but also to A_{1g} compressions. The only relevant parameter of the model is the ratio C^2/c_{44}^0 . The two order parameters of the model, $\Delta\alpha$ and s , are proportional to each other. The temperature dependence of the elastic constant c_{44} in the cubic phase is obtained as $c_{44}(T) = c_{44}^0 - C^2/3T$, an expression which is equivalent to the one we used in previous publications [4, 5].

The free parameter of the model is adjusted to yield a transition temperature of 186 K. The temperature dependences resulting for the order parameter and the elastic constant are shown as solid lines in Fig. 4. Also included is the construction for the temperatures $T_0 = 153$ K and $T_1 = 190$ K characteristic for a first order phase transition. T_0 and T_1 are the theoretical limits of the hysteresis effects. T_0 is the temperature where $c_{44}(T)$ would vanish if the phase transition were of second order.

The model describes the experimental results remarkably well, a fact which underlines that the mechanism of the phase transition is rather simple. In particular it suggests that the interactions in E_g symmetry are of secondary importance. Thus the ferroelastic transition in CsCN is more transparent than in KCN and NaCN where both symmetry strains, T_{2g} and E_g , are involved in the structural phase transition and where the easy direction of the

(CN)⁻ ions changes from $\langle 111 \rangle$ to one of the former $\langle 110 \rangle$ directions. The behaviour of the CN molecules in CsCN at lower temperatures is less well understood. The absence of a specific heat anomaly [3] and the absence of a Curie-Weiß-type behaviour of $\varepsilon_0(T)$ in the rhombohedral phase are strong arguments that there is no long range order of the CN dipoles. The (CN)⁻ ions seem to freeze into random occupations of the $[111]$ and $[\bar{1}\bar{1}\bar{1}]$ directions before a collective long range electric order, induced by dipolar intramolecular forces, can develop. The same situation was encountered in RbCN [11] whereas KCN and NaCN order anti-ferroelectrically [12]. Obviously the ratio of the dipole-dipole interaction to the hindering barrier E is slightly more favourable in the two latter compounds so that the fluctuations of the dipole system can evolve more freely down to the ordering temperature. Taking into account that the energy barriers E and the interatomic distances $r_{\text{CN-CN}}$ in CsCN and KCN are almost identical one must conclude that CsCN is just on the verge between dipole ordering and freezing into random CN-orientations. This view might be supported by the fact that $\varepsilon_0(T)$ as evaluated from the present data is falling with temperature (Fig. 6b), reminding us more on the results of the ordering system KCN [12] than on the freezing system RbCN [11].

References

1. Lely, J.A.: Thesis, Utrecht, 1942 (unpublished)
2. Natta, G., Passerini, L.: Gazz. Chim. Ital. **61**, 191 (1931)

3. Sugisaki, M., Matsuo, T., Suga, H., Seki, S.: Bull. Chem. Soc. Jpn. **41**, 1747 (1968)
4. Loidl, A., Knorr, K., Kjems, J.K., Haussühl, S.: J. Phys. **C13**, L349 (1980)
5. Loidl, A., Haussühl, S., Kjems, J.K.: Z. Phys. B - Condensed Matter **50**, 187 (1983)
6. Klein, M.L., Ozaki, Y., McDonald, I.R.: J. Phys. **C15**, 4993 (1982)
7. Lüty, F.: In: Defects in insulating crystals. Turkevitch, V.M., Svarts, K. (eds.). Berlin, Heidelberg, New York: Springer Verlag 1981
8. Shinnaka, Y., Yamamoto, S., Suematsu, Y.: J. Phys. Soc. Jpn. **43**, 1968 (1977)
9. Blat, D.Kh., Zinenko, V.I.: Sov. Phys. JETP **52**(3), 495 (1980)
10. Raedt, B. De, Binder, K., Michel, K.H.: J. Chem. Phys. **75**, 2977 (1981)
11. Kondo, Y., Schoemaker, D., Lüty, F.: Phys. Rev. **B19**, 4210 (1979)
12. Julian, M., Lüty, F.: Ferroelectrics **16**, 201 (1977)

G. Knopp
K. Knorr
A. Loidl
Institut für Physik
Universität Mainz
Jakob-Welder-Weg 11
D-6500 Mainz
Federal Republic of Germany

S. Haussühl
Institut für Kristallographie
Universität zu Köln
Zülpicher Strasse 49
D-5000 Köln 41
Federal Republic of Germany